Nanoscale

Accepted Manuscript

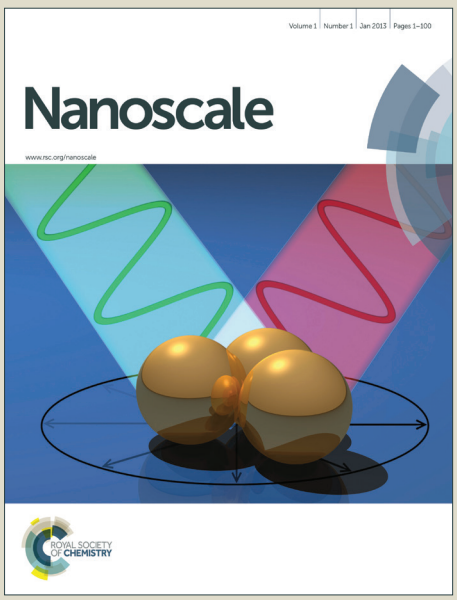

ROYAL SOCIETY OF CHEMISTRY

www.rsc.org/nanoscale

ARTICLE TYPE www. rsc.org/xxxxxx | XXXXXXXX

Metallic influence on the atomic structure and optical activity of ligand-protected nanoparticles: a comparison between Ag and Au

Francisco Hidalgo[a], Cecilia Noguez*[a], and Monica Olvera de la Cruz[b]

Received Xth XXXXXXXXXX 20XX, Accepted Xth XXXXXXXXX 20XX
First published on the web Xth XXXXXXXXXX 200X
DOI: 10.1039/b000000x

Using time-perturbed Density Functional Theory the optical activity of metal-thiolate compounds formed by a high symmetric Ag and Au nanoparticles (NPs) and a methyl-thiol molecule is studied after performing atomic optimizations and electronic calculations upon adsorption. Many different sites and orientations of the adsorbed molecule on icosahedral Ag and Au NPs of 55 atoms are considered. Upon molecule adsorption atomic distortions on Au NPs are induced while not on Ag, which causes larger molecule adsorption energies in Au than in Ag. Structural distortions and the specific molecule adsorption site and orientation result in chiral metal-thiolate NPs. Ag and Au compounds with similar chirality, according to Hausdorff chirality measurements, show different optical activity signatures, where circular dichroism spectra of Au NPs are more intense. These dissimilarities are attributed in part to the differences on the electronic density of states, which are a consequence of relativistic effects and the atomic distortion. It is concluded that optical activity of Ag and Au compounds are due to different mechanisms, while in Au is mainly due to the atomic distortion of the metallic NP induced after molecule adsorption, on Ag it is defined by the adsorption site and molecule orientation respect to the NP symmetry.

1 Introduction

In recent years a growing research interest has been paid in metal nanoparticles (NPs), including the synthesis and isolation, studies on the structure and electronic and optical properties, and the development of various applications, as well as the theoretical work and computing nanoparticles properties.[1–10] Metal nanoparticles composed of a specific number of atoms are of fundamental importance for investigating atomic structures, adsorption process, electronic and optical properties that can be eventually understood.[11–13] In particular, metal-thiolate nanoparticles exhibit interesting properties that can be manipulated by controlling different parameters, like size, shape, number of adsorbed thiols, which hold promise in a wide range of applications, such as catalysis, sensing, fluorescence labeling, and so forth.[14–18] Research works on the structure and bonding, chirality, ligand symmetry equivalence, catalysis, and photoelectrochemistry, etc. of metal-thiolate nanoparticles have revealed some particularly interesting aspects of their fundamental properties.[1–18] However, the role that the metallic part plays in the molecule adsorption process, and in their structural, electronic and optical properties has not been ultimately understood.

It has been observed that ligand-protected metallic nanoparticles have an exceptional optical activity that is contrasting to those of the components: ligands and nanoparticles.[9] Adsorption of organosulfur (SR) molecules on metal NPs could offer the possibility to create strong optical activity in the visible region.[19–22] Circular dichroism (CD) is a preferred tool for characterizing optical activity of chiral systems, which measures slight differences existing in optical extinction between left and right circularly-polarized light passing through chiral substances.[23] CD has a moderate sensitivity, which hampers the analysis at low concentrations and/or low enantiomeric excess. Controlled CD signals from organic molecules by using metallic NPs is desirable for having an enhancement mechanism of the optical activity. The latter might improve chiroptical spectroscopic techniques, which are useful to study molecule-molecule and molecule-nanostructure chiral interactions, which are of great significance since most molecules relevant in life are chiral. Thus, organometallic compounds have emerged in recent years as interesting nanoscale systems that hold promise in a wide range of applications, including molecular recognition.[24]

Enhancement of the CD spectra coming from the ligands has been observed to increase as the size of Ag NPs does.[25] To explain this, it has been proposed that surface plasmons supported by the metal NP enter in resonance with electronic transitions of the ligands involved in optical activity.[26,27] However, it is not clear until now how much this effect enhances the signal from the molecule, and even more if this is the

[a]*Instituto de Física, Universidad Nacional Autónoma de México, Apartado Postal 20-364, México D. F. 01000, México. Fax: +52 55 5616 1535; Tel: +52 55 5622 5106; * Corresponding author. E-mail: cecilia@fisica.unam.mx*
[b]*Department of Materials Science and Engineering, Northwestern University, Evanston, Illinois 60208, United States*

only mechanism. There might be other factors associated to NPs and ligands that could contribute besides NPs size.[28] For example, as the NP size increases the number of ligands adsorbed on it also does, and an augmentation of the CD signal is expected. However, there are other subtle effects that are related to the structure and bonding of the metallic NP and the molecule.[29–33] In the last few years, experiments have been performed in a variety of Ag and Au NPs and using different ligands to study optical activity.[19,20,34–39] In these experiments, the dependence with the kind of ligands, ligand concentration, the influence of the metallic species,[25] temperature dependence,[40] as well as the time evolution have been reported.[25] On the other hand, different mechanisms have been proposed to explain the observed optical activity, including an intrinsic chiral metallic core model,[19] a dissymmetric field model[20] originated from ligands protecting NPs, as well as the concurrency of both mechanisms.[35]

All these results in Au and Ag ligand-protected NPs show a complicated relationship between the resulting optical activity of a compound and its components. In this paper, we are interested in explain the influence of the metallic nature of the NP on the chiroptical signals, and the relationship with possible enhancement mechanisms. Here, we employ a single achiral molecule adsorbed at different sites and with different orientations on Ag and Au NPs. Our goal is to find how CD spectra are modulated by geometrical end electronic interactions inherent to each metal. Therefore, we also study in detail the atomic and electronic properties of the optimized compounds, where it is expected to find important differences because of strong relativistic effects present on Au. We anticipate that elucidating the main differences on the atomic, electronic, and optical activity could help to identify advantages that let make the selection between Ag and Au NPs, depending on specific requirements.

2 Methodology

2.1 Atomic models

We consider Au and Ag NPs composed by 55 atoms with icosahedral symmetry, which are optimized with a molecular dynamics procedure described below. In both cases, Ag_{55} and Au_{55}, the icosahedron is composed by a central-atom, where the center of mass is located. Then, the rest 54 atoms are distributed in two shell at three different distances respect to the central atom. These characteristic distances are given by the number of first-neighbor atoms, labeling each kind of atom by a well defined coordination number. The first or inner shell around the central atoms is composed by 12 atoms, all having 12 nearest atoms, such that their coordination number is (12). All the atoms at the inner shell are located at the same distance from the central atom. Therefore, the central atom also has coordination (12). The second or outer shell is composed by 42 atoms, where 12 atoms are at the vertices of the twenty triangular faces that compose the icosahedron. These 12 vertex atoms have coordination (6). The remaining 30 atoms form the edges of the triangular faces and have coordination (8). A schematic model is shown in Figure 1. The average distances in the optimized Ag_{55} from the central atom are 2.79, 4.82 and 5.52 Å, for core, edge and vertex atoms, respectively; while for Au_{55} are 2.78, 4.87, and 5.52 Å. Even that Au atoms are heavier than Ag, bond lengths are quite similar in both NPs, because the strong relativistic effects present in Au.[41,42]

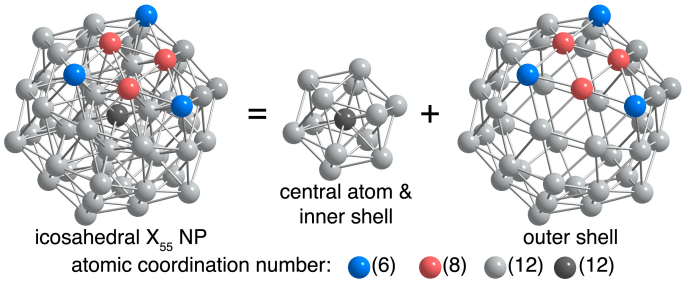

Fig. 1 Icosahedral NP of 55 atoms of element X(=Au or Ag) composed by twenty equivalent triangular faces, where one is remarked with atoms in blue and salmon colors to label the corresponding coordination number or first-neighbor atoms.

We assume that a SCH_4 molecule is adsorbed at the NP surface of X_{55} with X=Au or Ag. The thiol group on the metallic surface is adsorbed through the Sulfur (S) atom and one H atom is detached, SCH_3. Both, the X_{55} NP and SCH_4 molecule are achiral, so separately they do not show any optical activity. Due to the symmetry of bare X_{55} there are six possible adsorption sites for the achiral SCH_3 organic molecule: on the top of a metallic atom that can be located at the vertex [Top-Vertex(6)] shown in Figure 2(a), or the metallic atom that can be located at the edge [Top-Edge(8)] shown in Figure 2(b); between two metallic atoms located at the edge [Bridge Edge (6)-(8)] shown in Figure 2(c), or between two atoms located at the face [Bridge Face (8)-(8)] shown in Figure 2(d). There is also the possibility to adsorb the molecule on the middle between three atoms at the edge [Hollow-Edge (8)-(6)-(8)], and on the middle between three atoms at the face [Hollow-Edge (8)-(8)-(8)]. However, hollow configurations upon relaxation experiment drastic changes in the position of the molecule, ending in bridge cases. Therefore, the cases of adsorption sites reduce to Top-Vertex(6), Top-Edge(8), Bridge Edge (6)-(8), and Bridge Face (8)-(8), which are shown in Figure 2. Here the numbers in parenthesis denote the coordination number of the atoms involved in the adsorption process for each case. From these initial atomic arrangements many different molecule orientations around the adsorption site are considered, so the corresponding lowest-energy configurations are

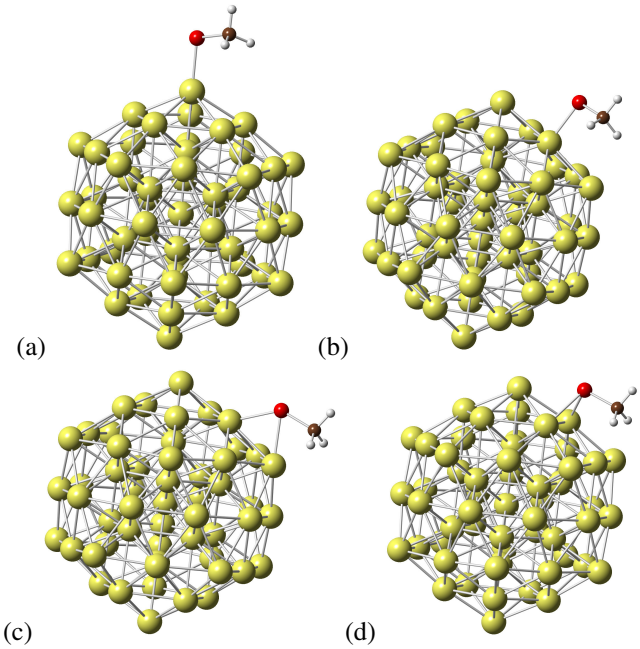

Fig. 2 (a) Top-vertex, (b) top-edge, (c) bridge-edge, and (d) bridge-face initial atomic arrangements of $X_{55}SCH_3$ are shown.

obtained by inspecting few hundreds of initial configurations by performing *ab initio* molecular dynamics simulations, as described next.

2.2 Computational details

Molecular dynamics simulations are performed using density functional theory (DFT), where general-gradient approximation (GGA) and Perdew-Burke-Ernzerhof (PBE) exchange-correlation functional are employed, as well as scalar-relativistic norm-conserving pseudopotentials. A double-ζ polarized basis set of numerical atomic orbitals is considered. Then, optimized lowest-energy configurations are obtained by considering unconstrained relaxations with atomic forces of 0.01 eV/Å, or less.[43] DFT calculations were performed using the SIESTA code,[44] which has been tested in many different Ag and Au NPs, both bare and ligand-protected.[30,34,45–47] The remarkable success of this kind of DFT methods in the structure prediction of $Au_m(SR)_n$ clusters has been recently discussed elsewhere.[48] Once the optimized atomic configurations and electronic states are found, circular dichroism (CD) spectra are calculated as follow. CD is an optical property that only chiral objects exhibit, and *ab initio* computations are necessary for its reliable interpretation. Using time-perturbed quantum-mechanical expressions, it is found that CD is directly related with the alignment of electric and magnetic dipole moments, i.e., the non-zero inner product of the matrix elements, $\langle 0|\vec{\mu}\cdot\vec{m}|n\rangle$. Here, $|0\rangle$ and $|n\rangle$ correspond to occupied and empty electronic states and $\vec{\mu}$ and $\vec{m}$ are the electric and magnetic dipole moment operators, respectively.[49] Due to the large number of atoms in nanostructures, first-principles CD calculations are computer demanding. A few years ago, we implemented in the DFT SIESTA code[44] the computation of CD spectra for large nanostructures.[50] This implementation allows us to take into account a larger number of electronic transitions, providing excellent results in agreement with experiments and other higher-level calculations done in small systems, such as CD spectra obtained from time-dependent DFT in chiral molecules.[50–52]

In the next section, we first discuss the structural differences between Ag and Au after optimization. Then, the lowest-energy configuration for each case is obtained. To compare equivalent $Au_{55}-SCH_3$ and $Ag_{55}-SCH_3$ NPs, we employed the Hausdorff chirality measure, which not only accounts for the atomic distortion but also for symmetry breaking upon adsorption. Hence, we discuss the calculated optical absorption and CD spectra, in terms of the relaxed atomic configurations and their corresponding electronic density of states.

3 Results and discussion

In the absence of the molecule, both NPs Ag_{55} and Au_{55} remain symmetric upon relaxation. This is observed in Table 1, where the mean distance, $\overline{R}$ of the core, vertex and edge atoms, as well as their corresponding standard deviations, σ, are reported. We observed that σ values are closed to zero, which indicates that in both NPs symmetry is conserved after optimization. It is also found that $\overline{R}$ values for Ag_{55} and Au_{55} are the same within a small difference of less than 1%, where the main variation is found for edge and vertex atoms both located at the outer layer. Despite that Au atoms are heavier than Ag ones, bond lengths on Au_{55} are quite similar to those on Ag_{55}. This fact has been attributed to the strong relativistic effects present on Au.[41,42] These structural differences and similarities between Ag and Au NPs are in agreement with those discussed previously.[30]

Here, only the lowest-energy configurations for both top and bridge adsorption sites are reported. When the molecule adsorption causes a chiral configuration of $Au_{55}-SCH_3$ or $Ag_{55}-SCH_3$, we have also examined the corresponding enantiomer to double-check results, since energy and $\overline{R}$ and σ values of both enantiomers should be the same. However, in this work we only report one enantiomer. In Table 1, $\overline{R}$ and σ of $Au_{55}-SCH_3$ and $Ag_{55}-SCH_3$ for top-vertex, top-edge, bridge-edge, and bridge-face cases, are also reported. Comparing $\overline{R}$ and σ for each $Au_{55}-SCH_3$ compound respect to bare Au_{55}, strong distortions in the NP are observed. For example, $\overline{R}$ and σ for the three kind of atoms in the compound

Table 1 Mean distance $\overline{R}$ and standard deviation σ in Å, for core, edge and vertex atoms in bare and molecule adsorbed Au and Ag NPs.

Ag	core $\overline{R}$ (σ)	edge $\overline{R}$ (σ)	vertex $\overline{R}$ (σ)	Au	core $\overline{R}$ (σ)	edge $\overline{R}$ (σ)	vertex $\overline{R}$ (σ)
Bare	2.79 (0.00)	4.82 (0.01)	5.52 (0.01)	Bare	2.78 (0.01)	4.87 (0.00)	5.52 (0.00)
Top-vertex	2.79 (0.02)	4.82 (0.02)	5.53 (0.04)	Top-vertex	2.79 (0.03)	4.87 (0.03)	5.53 (0.04)
Top-edge	2.79 (0.01)	4.82 (0.02)	5.53 (0.01)	Top-edge	2.79 (0.01)	4.88 (0.03)	5.52 (0.02)
Bridge-edge	2.79 (0.01)	4.82 (0.02)	5.53 (0.02)	Bridge-edge	2.79 (0.02)	4.89 (0.05)	5.52 (0.03)
Bridge-face	2.79 (0.01)	4.82 (0.02)	5.53 (0.01)	Bridge-face	2.79 (0.03)	4.90 (0.05)	5.53 (0.04)

are larger than those in Au_{55}, evidencing changes in the atomic distance distribution, as well as a symmetry breaking. Additionally, σ values of Au are larger than those for Ag, showing that Au−S interactions are stronger than the corresponding with Ag,[53] driving to larger atomic distortion in Au NPs. This fact is confirmed by comparing the adsorption energies reported in Table 2. The adsorption energy is calculated as the energy difference between the compound and the one of NP and molecule separated. This is

$$E_{ads} = E_{\text{NP-SCH}_3} - [E_{\text{NP}} + (E_{\text{SCH}_4} - 1/2E_{\text{H}_2})].$$

Here, $1/2E_{\text{H}_2}$ is the energy of the detached H atom from the SCH_4 molecule upon adsorption. Thus, it is found that molecule adsorption is more favorable in Au rather than in Ag by about 15% to 30%, being the largest difference for the bridge-face configuration. This is in agreement with the large electron affinity in metals and particularly in Au.[42] Additionally, by looking the results for Au top and bridge cases, we found that the trends in the adsorption energy and structural properties are similar to those obtained previously for Ag,[46] where it was found that top-vertex cases are independent of the SCH_3 orientation, while top-edge and both bridge cases exhibit a larger dependence. Also, the overall lowest-energy configuration in both Ag and Au is obtained for the bridge-face case.

Notice that $\overline{R}$ and σ are average properties, and the deviation for some atoms are difficult to observe. Therefore, to study in detail the displacement of Au or Ag atoms upon molecule adsorption in the NP, it is important to plot the distance of each atom respect to the central one. As an example in Figure 3 the bridge-face case is shown. Here, the average distance of bare NPs are shown in dashed lines. In Ag NPs, we find that core atoms remain very close to their original positions, as well as vertex atoms, while edge atoms are slightly deviated. On the other hand, Au atoms show important deviations from original positions, being more important in edge atoms. These observations are in agreement with the σ values reported in Table 1. In conclusion, it is evident that Au NPs suffer larger atomic distortions than Ag NPs after molecule adsorption. Chiral configurations were found for all lowest-energy compounds. In Table 2 also structural parameters related to the molecule adsorption are reported, like Au−S and

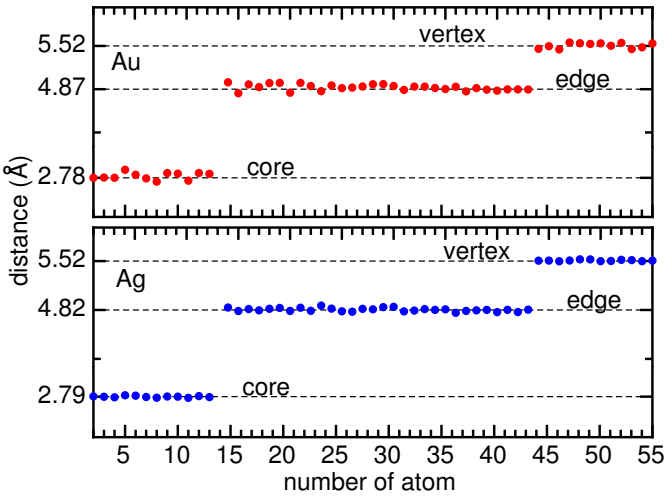

Fig. 3 Distances from the central atom for Au (red dots) and Ag (blue dots) atoms in the bridge-face case. Dashed lines show the average distance for bare NPs.

Ag−S bond lengths for top and bridge cases involving one and two metal atoms, respectively. In general, the distances between Ag−S are slightly larger than Au−S by about 1%. Additionally, top cases show shorter bond lengths than bridge cases. The angle formed by S−C and the metallic atom are quite similar for Au and Ag, and in general they show the same trends. However, by inspecting data from Tables 1 and 2, we notice a larger distortion for Au NPs upon adsorption by using a single SCH_3 ligand. This distortion could be related to the gain of the adsorption energy of the thiol group on Au. In fact, it has been observed that Au NPs passivated with multiple ligands, the strong Au−S interaction is able to distort the high symmetry of the NP to create novel structural motifs.[54–56]

To quantify the distortion of chiral arrangements, we employ the Hausdorff chirality measure,[57] $\overline{H}$, for each Ag_{55}−SCH_3 and Au_{55}−SCH_3 case, labeled as $\overline{H}_{com}$ in Table 3. $\overline{H}$ takes values between 0 and 1, where $\overline{H} = 0$ means that the system is achiral, and as $\overline{H}$ increases means that the system is far away from its mirror image being more chiral. A

Table 2 Structural properties and adsorption energy of $Au_{55}-SCH_3$ and $Ag_{55}-SCH_3$ top and bridge low-energy cases.

Case	Au-S (Å)	Au-S-C (deg)	E_{ads} ($Au_{55}-SCH_3$) (kcal mol^{-1})	Ag-S (Å)	Ag-S-C (deg)	E_{ads} ($Ag_{55}-SCH_3$) (kcal mol^{-1})
top-vertex	2.36	103.9	9.33	2.38	103.0	7.11
top-edge	2.35	102.6	18.60	2.39	105.3	13.17
bridge-edge	2.47/2.43	106.5/103.7	30.89	2.50/2.50	107.1/100.7	26.36
bridge-face	2.45/2.47	104.7/108.2	37.07	2.50/2.52	106.7/112.4	29.44

brief description of the Hausdorff method to measure chirality and its significance is given in Reference [58]. Here, we found that bare Ag_{55} and Au_{55} have $\overline{H} = 0.000$, in agreement with the fact that both are achiral. It is observed that $\overline{H}_{com}$ values for Ag and Au are slightly different as comparing for each case, being larger for Au compounds. However, to investigate the NP atomic arrangement distortion, we also compute the Hausdorff chirality measurement for just the metallic part or NP, denoted by $\overline{H}_{NP}$ also reported in Table 3. These values are in agreement with the differences in the standard deviation, σ, of the atomic positions of the metallic NP reported in Table 1. The non-zero value for Ag and Au $\overline{H}_{NP}$ means that upon molecule adsorption, chirality is induced on the NP. Additionally, this induced chirality is larger in Au than in Ag, actually Ag NPs remain fairly symmetric after molecule adsorption with $\overline{H}_{NP} \leq 0.08$. This induced chirality upon passivation in Au NP was reported and discussed widely by Garzón and coworkes.[38,59] They found that when a highly symmetric Au_{38} NP, with $\overline{H}_{NP} = 0.000$, is passivated with 24 SCH_3 molecules or ligands, the final system exhibits a $\overline{H}_{NP} = 0.121$, which is larger in comparison with the values obtained here, probably because the large difference on the number of molecules adsorbed.

Table 3 Hausdorff chirality measure of low-energy $Ag_{55}-SCH_3$ and $Au_{55}-SCH_3$ cases.

	$Ag_{55}-SCH_3$		$Au_{55}-SCH_3$	
Case	$\overline{H}_{com}$	$\overline{H}_{NP}$	$\overline{H}_{com}$	$\overline{H}_{NP}$
top-vertex	0.046	0.002	0.046	0.008
top-edge	0.064	0.002	0.076	0.005
bridge-edge	0.083	0.008	0.093	0.028
bridge-face	0.051	0.006	0.065	0.018

Within the DFT scheme, the imaginary part of the dielectric function is calculated for Au_{55}, top and bridge $Au_{55}-SCH_3$ cases, and they are compared with the corresponding Ag configurations reported previously.[46] For a full description of the optical properties, a many-body description would be desirable.[60] However, our results are in good agreement with trends found using time-dependent DFT (TDDFT) calculations done in bare Au and Ag small clusters,[61] where general directions can be drawn. Also, we found a good agreement with a recent TDDFT calculation of the optical absorption of Au_{55}. In Figure 4, we compare the optical absorption obtained from the dielectric function of Au_{55}, and the one calculated using TDDFT.[62] Since DFT underestimates the energy of empty states, we have shifted the DFT spectrum by about 1 eV to make easier the comparison with the TDDFT calculation. Details of how optical absorption is calculated from the dielectric function are in Reference [63]. However, the discussion of the optical properties below is done using the imaginary part of the dielectric functions, since more details can be appreciated.

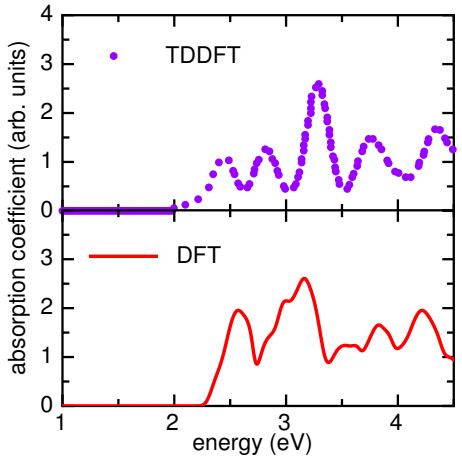

Fig. 4 Imaginary part of the NPs dielectric function as a function of energy. Optical absorption spectra for Ag NPs are in blue lines, while for Au are in red lines. Top plot shows results for bare NPs. Middle and bottom plots show spectra for top and bridge cases, respectively.

Top plot in Figure 5 shows NPs imaginary part of the dielectric function for bare Au_{55} and Ag_{55}, which exhibit similar behavior. For instance, the well-defined peak structure of the spectra is associated to transitions between molecular-like electronic states which are highly degenerated because of the 5-fold symmetry of Au_{55} and Ag_{55}. Here, optical absorption starts just below 1.5 eV, where an intense peak is observed, being larger for Ag than Au NPs. Another structure is found centered at about 2.0 eV, which are half intense than the peak

at lower energy, and their line shapes show small differences associated to the distribution of the density of states described in Figure 6. Above 2.5 eV, an extended tail is found that also show a peak structure but with smaller intensity. However, at such energies the absorption spectra is slightly more intense now in Au_{55} than in Ag_{55}.

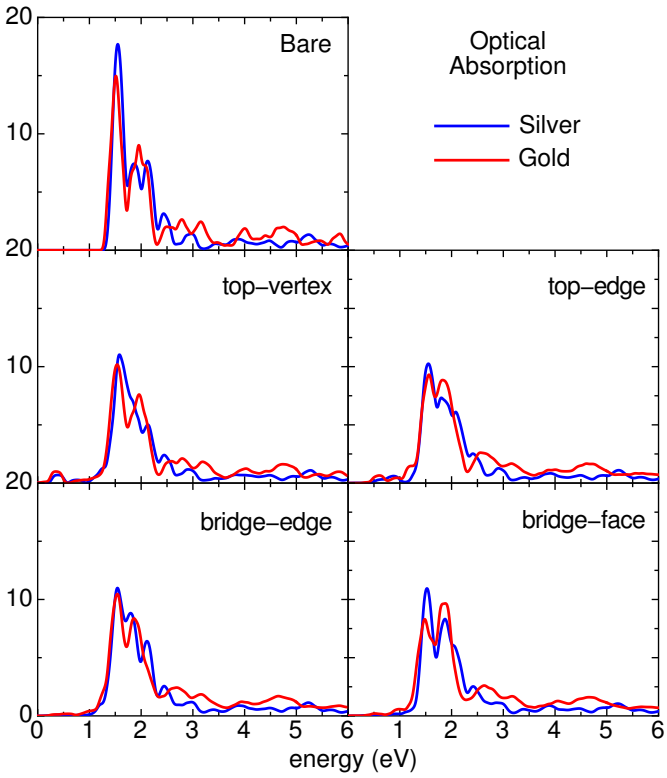

Fig. 5 Imaginary part of the NPs dielectric function as a function of energy. Optical absorption spectra for Ag NPs are in blue lines, while for Au are in red lines. Top plot shows results for bare NPs. Middle and bottom plots show spectra for top and bridge cases, respectively.

The optical response is dictated by the electronic density of states (DOS) of each system. Figure 6 shows different contributions to DOS of Au_{55} and Ag_{55} from each kind of atom identified by its coordination number, i.e. contributions from core (12), edge (8), and vertex (6) atoms are displayed in green, blue, and yellow, respectively. Here, the Fermi level is set to 0 eV. Both bare NPs exhibit molecular-like electronic states due to quantum-size effects. Additionally, these states are degenerated because the high symmetry of icosahedral NPs. These two facts are more evident for Ag, where electronic states are at well-defined energies between -2.5 and 2.5 eV. These localized states give rise to electron transitions with specific energies, which result in an absorption spectrum with a well-defined structure. For instance, in Ag_{55} electron transitions from occupied states at about -0.6 eV to empty states around $+0.9$ eV, are responsible for the absorption band located at 1.5 eV. The optical band with two shoulders centered 2.0 eV comes from transitions between occupied and empty states at -0.9 and $+0.9$ eV; and between -0.6 and $+1.6$ eV. Additionally, we have identified the occupied states at -0.6 and -0.9 eV with mainly $5s$ orbitals, although $4d$ orbitals are also present but in small quantity. On the other hand, empty states at $+0.9$ and $+1.6$ eV have similar contributions from both $5s$ and $5p$ orbitals. Below -2.5 eV DOS increases and becomes continues, because of the dominant presence of $4d$ occupied states at such energies. Transitions from these states to empty ones are responsible of the tail in the optical spectrum described above.

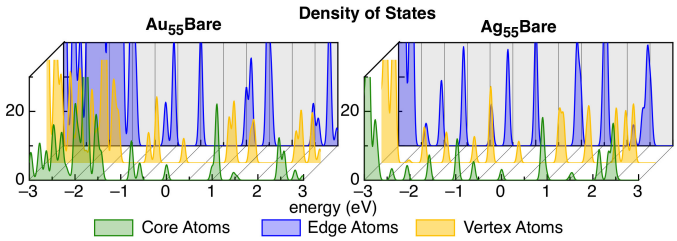

Fig. 6 Contributions to DOS in arbitrary units from core, edge, and vertex atoms are shown in green, blue and yellow, respectively. The contribution are slightly displaced to facilitate the comparison. Results for bare Au_{55} and Ag_{55} are shown at the left and right hand side, respectively. The Fermi level is at 0 eV.

Now, let us discuss the case of Au that is different mainly due to strong relativistic effects. Comparing with Ag, occupied states at -0.9 eV are now slightly shifted to -0.75 eV, such that they are very close to those occupied states at -0.6 eV. An important difference is that now both occupied states have similar contributions from $5d$ and $6s$ orbitals, showing different character from the corresponding ones in Ag. The empty states at $+0.9$ eV in Ag are slightly shifted in Au to about $+1.1$ eV and the orbital character is still the same, i.e., they are similar contributions of $6s$ and $6p$ orbitals. Finally, occupied states at energies below -1.5 eV show a much larger contribution for Au than in Ag, because of the dominant presence of $5d$ occupied states at such energies, while in Ag $4d$ states are dominant below -2.5 eV . These differences between Au and Ag arise from relativistic effects more present in Au, which are raising the $5d$ orbitals.[41] These differences in DOS produce some variations in optical absorption when comparing spectra of both NPs. For example, we found that below 2.5 eV the spectrum of Au is less intense than Ag, because of the partly lost of DOS peak sharpness. Additionally, the double-peak optical band centered 2 eV in Ag now is lost for Au, because of the energy shift of the involved occupied and empty electronic states, giving a similar structure but with

slightly different line shape. Finally, at energies larger than 2.5 eV optical absorption is now more intense for Au than in Ag, because the presence of *d* orbitals.

Figure 5 displays the imaginary part of the NPs dielectric function after molecule adsorption, where only spectra of lowest-energy top and bridge cases are shown in middle and bottom plots, respectively. Despite the atomic distortion induced on Au NPs but not in Ag, optical spectra show quite similar behavior. Upon molecule adsorption the NP electronic degeneracy is broken, spreading occupied and empty electronic states at higher and lower energies giving rise to electron transitions below 1.5 eV of low intensity. All configurations optical absorption spectra with discrete peaks. The intensity of the optical peak at 1.5 eV is diminished by about 40%, but it is still more intense for Ag than Au. Similar trends in optical absorption response have been already found by Aikens,[61] who employed time-dependent DFT in Ag_{25} and au_{25} ligand-protected NPs, as well as in mixed metal "core-shell" configurations. For instance, the discrete peak structure of spectra of Ag and Au NPs is similar, being more intense for Ag.

Again, the main optical bands can be explained by looking at the DOS for each case, shown in Figure 7. Additionally to the different contributions to DOS from core (green), vertex (blue) and edge (yellow) atoms of the metallic NPs, the contribution from the S atom is also shown in red. Top row of Figure 7 displays DOS for Au compounds, while the corresponding $Ag_{55}-SCH_3$ compounds are in the bottom row. Sulfur electron states are mainly $3p$ and are extended over a wide energy range below the Fermi level, which means that they are occupied. It is observed that the main differences in the absorption spectra can be followed by looking at the contribution from the S atom. For instance, for both top cases we found that the spectra is mainly modified between 0.5 and 2.0 eV. This means that the electronic states, discussed above, at -0.6 and -0.9 eV are now modified by the presence of the molecule, since S states are more localized around these energies. On the other hand, for both bridge cases the changes are found at all energies. Notice now that electron states from S atoms are less localized. It is remarkable the independence of DOS and thus, of optical absorption with the molecule orientation. As consequence, achiral and chiral configurations of the same case exhibit the same optical absorption, being impossible to distinguish between them. Nevertheless, chiroptical spectroscopies are able to account this structural property if the system is chiral, as it has been previously shown.[46]

Let us discuss the influence of the structural properties in the optical activity of Ag and Au compounds studied here. As expected, highly symmetric systems, i.e. bare NPs and the isolated molecule, exhibit null chiroptical signals. Additionally, we confirm that enantiomers show the same CD spectra but with opposite sign. We previously found that the most-stable $Ag_{55}-SCH_3$ isomers can be chiral or achiral under different SCH_3 orientations, and show quite different CD spectra, in contrast to optical absorption.[46] However, Au compounds are always chiral because the atomic distortion discussed above. In Figure 8, CD spectra of low-energy top and bridge cases are shown in red solid lines for Au, and in blue solid lines for Ag. Also, the corresponding $\overline{H}_{com}$ values are shown. We compare CD spectra for Ag and Au equivalent compounds that also exhibit similar $\overline{H}_{com}$ values. In general, Au compounds show more larger CD intensities than Ag ones, except for the top-edge case where intensities are similar. The differences in intensity are in agreement with the fact that $\overline{H}_{com}$ values of Au systems are slightly larger than Ag ones. Additionally, as larger $\overline{H}_{com}$ is the CD spectra become more intense in Au compounds. However, this is not found for Ag compounds. This latter suggest that the origin of optical activity might be different in Au than in Ag. Also, CD spectra of Ag and Au equivalent compounds are not similar among they, despite that their optical properties do. Furthermore, it is found that small $\overline{H}_{com}$ differences between Au and Ag result in large differences in CD intensities and line shapes. Additionally, both top-vertex cases show the same $\overline{H}_{com}$, but the CD spectrum of Au is about five times more intense than the one of Ag.

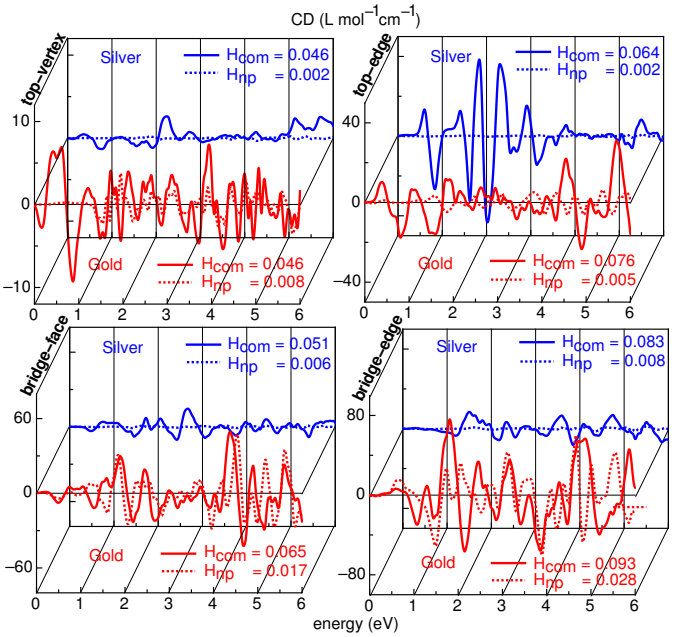

Fig. 8 CD spectra of top and bridge Au (Ag) compounds are shown in red (blue) line. While straight line refers to CD for $Au_{55}-SCH_3$ ($Ag_{55}-SCH_3$) compounds, doted line is CD from the respective Au (Ag) isolated NC. For each case, $\overline{H}_{com}$ and $\overline{H}_{nc}$ are included. Ag CD spectra were discussed previously[46].

These variations in CD line-shapes, intensities, and $\overline{H}_{com}$ values between similar Au and Ag compounds, give us some

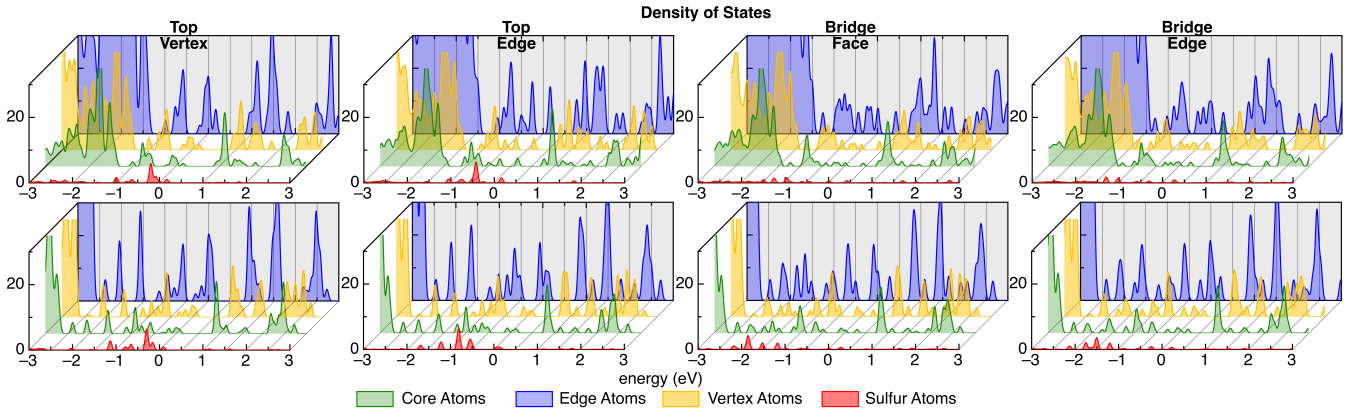

Fig. 7 Contributions to DOS in arbitrary units from core, edge, and vertex atoms are shown in green, blue and yellow, respectively, while contributions from S atom is in red. The contribution are slightly displaced to facilitate the comparison. Results for Au (top row) and Ag (bottom row) compounds of low-energy top and bridge cases. Fermi level is at 0 eV.

insights into the origin of the optical activity as a function of the metallic component of the NP. We previously found that in Ag systems the metallic part remains very symmetric, such that optical activity depends on the symmetry breaking given by the adsorption site and orientation of the molecule.[46] The adsorption site determines the line-shape and magnitude, while the molecule orientation tunes the intensitymaxima and minima. However, the mechanism for Au systems looks quite different. To elucidate this mechanism, we calculate CD spectra and the Hausdorff chirality measure for only the metallic part or $\overline{H}_{NP}$. In Figure 8 these spectra are shown dotted lines also in red and blue for Au and Ag NPs, respectively. As expected, Ag NPs exhibit null chiroptical signals corresponding to achiral atomic arrangements in agreement with the very small computed $\overline{H}_{NP}$ values. An opposite behavior is observed in Au compounds, now CD intensities with and without molecule are of the same order of magnitude. This means that the metallic part of Au compounds is mainly responsible of optical activity of the whole compound. This is in agreement with the large $\overline{H}_{NP}$ values for Au. Therefore, it is found that initial achiral Au NPs become chiral after molecule adsorption due to an atomic distortion of the NP, and their chiroptical signals are very similar to the whole compound. Despite $\overline{H}_{NP}$ values are smaller than $\overline{H}_{com}$ in Au compounds, the CD intensity and line shape is practically defined by the chirality induced on the metallic NP. Unlike Ag compounds, whose optical activity is defined by the absence of a common symmetry plane between the NP and molecule.[46]

To gain a better understanding in the CD line shapes, we can look again at the computed DOS of top and bridge $Au_{55}-SCH_3$ and $Ag_{55}-SCH_3$ cases. As we mentioned above, chiral and achiral isomers of a given case exhibit the same DOS, but different cases have different electronic distribution. DOS of Au and Ag systems in Figure 7 show strong electronic distortion, which is associated to the adsorption of the molecule. For instance, top cases have S electronic states that are more energetically localized than those found in bridge cases. In top cases, occupied S states are located above -1.0 eV, and the DOS discrete peak structure of Ag atoms in the bare NP is partly lost, while states below such energies remain quite unperturbed. On the other hand, bridge cases show a wider energy region around -1.7 eV where S occupied states are present. Notice that the Au$-$S interaction is different to that found in Ag, because it induces an atomic distortion in the metallic NP, so that it breaks notably the large degeneration of both occupied and unoccupied states, modifying the chiroptical response of both Au and Ag NPs.

4 Conclusion

The metallic influence on the atomic structure and optical activity was studied for Au and Ag icosahedral NPs, Ag_{55} and Au_{55}, before and after the adsorption of a SCH_3 molecule. Different adsorption sites were considered, as well as different molecule orientations respect to the NPs. Molecule adsorption is favored in both metals when the molecule is bond to two metal atoms forming a bridge. Low-energy metal-thiolate NPs show different atomic structure depending on the atomic specie. For instance, Ag NPs are minimally reshaped while Au NPs are more susceptible to be distorted due to the sulfur interaction. Thus, low-energy Au NPs become chiral just by the adsorption of a single SCH_3 molecule, while Ag NPs can be chiral or no depending on the molecule adsorption site and orientation. By comparing energies in both types of NPs, it is found that adsorption of the thiol group is favored up to 30% on Au rather than on Ag. Optical absorption spectra of bare metallic NPs are quite similar. The optical response is dominated by the high degeneracy of the electronic states, particu-

larly at low energies, while at larger energies some difference are found because relativistic effects more present in Au than in Ag NPs. Such effects are also responsible of the preference to adsorb the molecule in Au than in Ag. The optical response of NPs-molecule equivalent compounds are also quite similar for Ag and Au. In contrast, circular dichroism spectra are more sensitive to configurational changes, such as the adsorption site, molecule orientation, and distortion of the metallic NP.

An outstanding conclusion is that optical activity of Ag and Au compounds are due to different mechanisms. While CD spectra of Ag compounds arise from the off alignment between the symmetry planes of the Ag NP and the one of the SCH_3 molecule;[46] for Au compounds CD is mainly defined by the emerging chirality of the metallic part. Additionally, CD intensities of equivalent compounds are larger in Au than in Ag. This particular mechanism associated to Au compounds is in good agreement with theoretical other predictions,[19] and recent experimental results,[33] where using achiral ligands it was found that the influence of the ligand on the chiroptical spectra is minor. Hence, they observed strong structural contributions to CD spectra from Au compounds rather than chirality associated to ligands.

We anticipate that these two different mechanisms that give origin to optical activity can be employed for different applications. For example, large intensities can be achieved by using Au NPs and the line-shape is determined by the atomic distortion of the NP. On the other hand, Ag NPs can be more useful to control chiroptical signals from chiral ligands because the its atomic arrangement is unchanged, providing more information about the ligands. Additional studies about the relationship between optical activity of the metallic NP-molecule compounds in terms of NPs and number of ligands will contribute to understand the importance of each mechanism. It is expected that this work motivates to develop new experiments for improving control on the structural and optical properties of ligand-protected nobel metal NPs.

Acknowledgement

We acknowledge Prof. Ignacio L. Garzón to make available for use the Hausdorff chirality measure code. FH also acknowledge partial support from Northwestern University Materials Research Science and Engineering Center (NSF MRSEC program DMR-1121262) during a short visit. This work has been supported by DGAPA-UNAM PAPIIT IN104212-3 and CONACyT 179454 grants.

References

1 Y. Pei, Y. Gao and X. C. Zeng, *J. Am. Chem. Soc.*, 2008, **130**, 7830–7832.
2 M. J. Rodriguez-Valazquez, M. C. Blanco, R. Lourido, C. Vaazquez-Valazquez, E. Pastor, G. A. Planes, J. Rivas and M. A. Lopez-Quintela, *Langmuir*, 2008, **24**, 12690–12694.
3 P. Maity, S. Xie, M. Yamauchi and T. Tsukuda, *Nanoscale*, 2012, **4**, 4027–4037.
4 K. M. Harkness, Y. Tang, A. Dass, J. Pan, N. Kothalawala, V. J. Reddy, D. E. Cliffel, B. Demeler, F. Stellacci, O. M. Bakr and J. A. McLean, *Nanoscale*, 2012, **4**, 4269–4274.
5 H. Qian, Y. Zhu and R. Jin, *ACS Nano*, 2009, **3**, 3795–3803.
6 H. Qian, Y. Zhu and R. Jin, *J. Am. Chem. Soc.*, 2010, **132**, 4583–4585.
7 Y. Pei, N. Shao, Y. Gao and X. C. Zeng, *ACS Nano*, 2010, **4**, 2009–2020.
8 O. Lopez-Acevedo, H. Tsunoyama, T. Tsukuda, H. H. and C. M. Aikens, *J. Am. Chem. Soc.*, 2010, **132**, 8210–8218.
9 T. G. Schaaff and R. L. Whetten, *J. Phys. Chem. B*, 2000, **104**, 2630–2641.
10 A. Guerrero-Martínez, J. L. Alonso-Gómez, B. Auguié, M. M. Cid and L. M. Liz-Marzán, *Nano Today*, 2011, **6**, 381 – 400.
11 R. Jin, S.-K. Eah and Y. Pei, *Nanoscale*, 2012, **4**, 4026–4026.
12 M. W. Heaven, A. Dass, P. S. White, K. M. Holt and R. W. Murray, *J. Am. Chem. Soc.*, 2008, **130**, 3754–3755.
13 M. Zhu, C. M. Aikens, F. J. Hollander, G. C. Schatz and R. Jin, *J. Am. Chem. Soc.*, 2008, **130**, 5883–5885.
14 M. Haruta and M. Daté, *Appl. Catal., A*, 2001, **222**, 427 – 437.
15 M.-C. Daniel and D. Astruc, *Chem. Rev.*, 2004, **104**, 293–346.
16 E. S. Andreiadis, M. R. Vitale, N. Mezailles, X. Le Goff, P. Le Floch, P. Y. Toullec and V. Michelet, *Dalton Trans.*, 2010, **39**, 10608–10616.
17 T. Zhou, M. Rong, Z. Cai, C. J. Yang and X. Chen, *Nanoscale*, 2012, **4**, 4103–4106.
18 L. Shang, L. Yang, F. Stockmar, R. Popescu, V. Trouillet, M. Bruns, D. Gerthsen and G. U. Nienhaus, *Nanoscale*, 2012, **4**, 4155–4160.
19 C. E. Roman-Velazquez, C. Noguez and I. L. Garzon, *J. Phys. Chem. B*, 2003, **107**, 12035–12038.
20 M.-R. Goldsmith, C. B. George, G. Zuber, R. Naaman, D. H. Waldeck, P. Wipf and D. N. Beratan, *Phys. Chem. Chem. Phys.*, 2006, **8**, 63–67.
21 H. Yao, M. Saeki and K. Kimura, *J. Phys. Chem. C*, 2010, **114**, 15909–15915.
22 C. Noguez and I. L. Garzón, *Chem. Soc. Rev.*, 2009, **38**, 757–771.
23 N. Berova, K. Nakanishi and R. W. Woody, *Circular dichroism, principles and applications*, Wiley-VCH, New York, 2nd edn., 2000.
24 J. Liu, J. Alvarez and A. E. Kaifer, *Advanced Materials*, 2000, **12**, 1381–1383.
25 T. Li, H. G. Park, H.-S. Lee and S.-H. Choi, *Nanotech.*, 2004, **15**, S660.
26 A. O. Govorov, Z. Fan, P. Hernandez, J. M. Slocik and R. R. Naik, *Nano Lett.*, 2010, **10**, 1374–1382.
27 I. Lieberman, G. Shemer, T. Fried, E. Kosower and G. Markovich, *Angew. Chem. Int. Ed.*, 2008, **47**, 4855–4857.
28 C. Noguez, A. Sánchez-Castillo and F. Hidalgo, *J. Phys. Chem. Lett.*, 2011, **2**, 1038–1044.
29 C. M. Aikens, *J. Phys. Chem. Lett.*, 2011, **2**, 99–104.
30 E. M. Fernández, J. M. Soler, I. L. Garzón and L. C. Balbás, *Phys. Rev. B*, 2004, **70**, 165403.
31 J. W. Zwanikken, P. Guo, C. A. Mirkin and M. Olvera de la Cruz, *J. Phys. Chem. C*, 2011, **115**, 16368–16373.
32 P. Guo, R. Sknepnek and M. Olvera de la Cruz, *J. Phys. Chem. C*, 2011, **115**, 6484–6490.
33 I. Dolamic, S. Knoppe, A. Dass and T. Bürgui, *Nature Comm.*, 2012, **3**, 798.
34 F. Hidalgo, A. Sánchez-Castillo, I. L. Garzón and C. Noguez, *Eur. Phys. J. D*, 2009, **52**, 179–182.
35 A. Sánchez-Castillo, C. Noguez and I. L. Garzón, *J. Am. Chem. Soc.*, 2010, **132**, 1504–1505.
36 C. Gautier and T. Bürgi, *Chem. Phys. Chem.*, 2009, **10**, 483–492.

37 H. Yao, *Curr. Nanoscience*, 2008, **4**, 92–97.

38 I. L. Garzón, J. A. Reyes-Nava, J. I. Rodríguez-Hernández, I. Sigal, M. R. Beltrán and K. Michaelian, *Phys. Rev. B*, 2002, **66**, 073403.

39 T. Tsukuda, H. Tsunoyama and Y. Negishi, in *In Metal Nanoclusters in Catalysis and Materials Science: The Issue of Size Control*, Elsevier: Amsterdam, 2008, p. 373.

40 H. Yao, T. Fukui and K. Kimura, *J. Phys. Chem. C*, 2007, **111**, 14968–14976.

41 P. Pyykko and J. P. Desclaux, *Accounts Chem. Res.*, 1979, **12**, 276.

42 H. Schmidbaur, S. Cronje, B. Djordjevic and O. Schuster, *Chem. Phys.*, 2005, **311**, 151 – 161.

43 Additionally, we tested the force tolerance using smaller values than 0.005 eV/Å, confirming the convergence for all cases.

44 J. M. Soler, E. Artacho, J. D. Gale, A. García, J. Junquera, P. Ordejón and D. Sánchez-Portal, *J. Phys.: Cond. Matt.*, 2002, **14**, 2745.

45 X. Xing, R. M. Danell, I. L. Garzón, K. Michaelian, M. N. Blom, M. M. Burns and J. H. Parks, *Phys. Rev. B*, 2005, **72**, 081405.

46 F. Hidalgo and C. Noguez, *ACS Nano*, 2013, **7**, 513–521.

47 A. M. Angulo and C. Noguez, *J. Phys. Chem. A*, 2008, **112**, 5834–5838.

48 D.-e. Jiang, *Nanoscale*, 2013, **5**, 7149–7160.

49 L. D. Barron, *Molecular Light Scattering and Optical Activity*, Cambridge University Press, Cambridge, 2nd edn., 2004.

50 F. Hidalgo, A. Sánchez-Castillo and C. Noguez, *Phys. Rev. B*, 2009, **79**, 075438.

51 F. Hidalgo and C. Noguez, *phys. status solidi (b)*, 2010, **247**, 1889–1897.

52 A. Sánchez-Castillo and C. Noguez, *J. Phys. Chem. C*, 2010, **114**, 9640–9644.

53 T. Udayabhaskararao and T. Pradeep, *J. Phys. Chem. Lett.*, 2013, **4**, 1553–1564.

54 H. Häkkinen, M. Walter and H. Grönbeck, *J. Phys. Chem. B*, 2006, **110**, 9927–9931.

55 M. Walter, J. Akola, O. Lopez-Acevedo, P. D. Jadzinsky, G. Calero, C. J. Ackerson, R. L. Whetten, H. Grönbeck and H. Häkkinen, *P. Natl. Acad. Sci. USA*, 2008, **105**, 9157–9162.

56 H. Häkkinen, *Nature Chem.*, 2012, **4**, 443.

57 A. B. Buda and K. Mislow, *J. Am. Chem. Soc.*, 1992, **114**, 6006–6012.

58 We are interested in compare silver and gold compounds with similar chirality to elucidate how the metallic specie contributes to optical activity. We use a mathematical tool capable to quantify chirality based on molecular symmetry, independent of its physical and chemical manifestations. Hausdorff chirality measure[57] ($\overline{H}$) is employed to quantify, and thus to compare, chirality of $Ag_{55}SCH_3$ and $Au_{55}SCH_3$ compounds, in a similar way to those made by Garzón and coworkers to quantify chirality in bare and passivated Au NPs.[38,59] $\overline{H}$ is based on Hausforff's concept of distances between sets, in agreement with following notion: although a couple of enantiomorphs (molecules or any object) cannot be superposed by any rotation-traslation, they can be overlapped in such way that at least parts of them coincide. In this way, let Q and Q' denote two enantiomorphous, non-empty and bounded sets of points. The Hausdorff distance $h(Q,Q')$ between Q and Q' can be expressed as the smallest number $\delta = h(Q,Q')$, such that, a spherical ball of radius δ centered at any point of Q contains at least one point of Q', and vice versa, a spherical ball of radius δ centered at any point of Q' contains at least one point of Q. Hence, through a set of rotation-traslation operations, it is possible to find the maximal overlap between enantiomorphs, which can be associated directly as a measurement of their chirality, independently of their orientation. Such mathematical artifice should have the following properties: (a) be continuous, (b) normalized to the interval $[0,1]$, (c) equal to zero if and only if the enantiomorph is achiral, and (d) dependent on shape but not on size. It is necessary remark that we will assume that two compounds with similar $\overline{H}$ have similar chirality, but it does not mean that they exhibit similar optical activity, because it depends on its geometrical and electronic description. Hence, $\overline{H}$ is helpful to separate structural and electronic contributions from optical activity.

59 I. Garzón, M. Beltrán, G. González, I. Gutíerrez-González, K. Michaelian, J. Reyes-Nava and J. Rodríguez-Hernández, *Eur. Phys. J. D*, 2003, **24**, 105–109.

60 Electron transitions around the Fermi Level were not taken into account in the calculation of optical absorption. This means that intraband transitions are not considered.

61 C. M. Aikens, *J. Phys. Chem. C*, 2008, **112**, 19797–19800.

62 R. W. Burgess and V. J. Keast, *J. Phys. Chem. C*, 2011, **115**, 21016–21021.

63 The optical absorption coefficient, α is given in terms of the dielectric function as:

$$\alpha(\omega) = 2\frac{\omega}{n(\omega)c}\varepsilon''(\omega),$$

where c is the speed light, $n(\omega)$ is the refraction index, and $\varepsilon''(\omega)$ is the imaginary part of the dielectric function, with

$$n(\omega) = \sqrt{\frac{1}{2}[\varepsilon'(\omega) + \sqrt{\varepsilon'^2(\omega) + \varepsilon''^2(\omega)}}.$$

Here, $\varepsilon'(\omega)$, the real part of the dielectric function is obtained from the Kramers-Kronig relations. For a detail discussion the reader can consult Reference [64].

64 H. Haug and S. W. Koch, *Quantum Theory of the Optical and Electronic Properties of Semiconductors*, World Scientific, Singapore, 3rd edn., 1990.

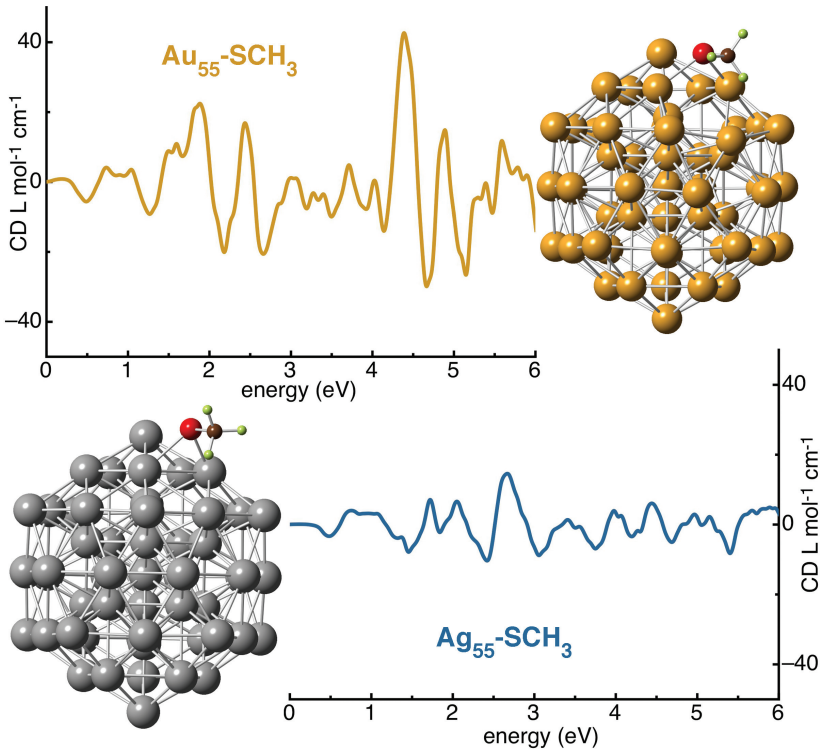

Fig. 9 Graphical abstract. Circular Dichroism spectra of gold and silver nanoparticles with one SCH_3 adsorbed molecule.

Table of contest entry

The metallic influence on atomic structure and optical activity was studied for Au and Ag NPs upon adsorption of SCH_3.